872 *Biochemistry* **2010,** *49,* 872–881
DOI: 10.1021/bi901751b

BIOCHEMISTRY
including biophysical chemistry & molecular biology
Article

The Ability of Rodent Islet Amyloid Polypeptide To Inhibit Amyloid Formation by Human Islet Amyloid Polypeptide Has Important Implications for the Mechanism of Amyloid Formation and the Design of Inhibitors[†]

Ping Cao,[‡] Fanling Meng,[‡] Andisheh Abedini,[§] and Daniel P. Raleigh*[,‡,∥]

[‡]*Department of Chemistry, State University of New York, Stony Brook, New York 11794-3400,* [§]*Division of Surgical Science, Department of Surgery, College of Physicians and Surgeons, Columbia University, New York, New York 10032, and* [∥]*Graduate Program in Biochemistry and Structural Biology and Graduate Program in Biophysics, State University of New York, Stony Brook, New York 11794*

Received October 11, 2009; Revised Manuscript Received December 21, 2009

ABSTRACT: Islet amyloid polypeptide (IAPP) is a 37-residue polypeptide hormone that is responsible for islet amyloid formation in type II diabetes. Human IAPP is extremely amyloidogenic, while rat IAPP and mouse IAPP do not form amyloid in vitro or in vivo. Rat IAPP and mouse IAPP have identical primary sequences, but differ from the human polypeptide at six positions, five of which are localized between residues 20 and 29. The ability of rat IAPP to inhibit amyloid formation by human IAPP was tested, and the rat peptide was found to be an effective inhibitor. Thioflavin-T fluorescence-monitored kinetic experiments, transmission electron microscopy, and circular dichroism showed that rat IAPP lengthened the lag phase for amyloid formation by human IAPP, slowed the growth rate, reduced the amount of amyloid fibrils produced in a dose-dependent manner, and altered the morphology of the fibrils. The inhibition of human IAPP amyloid formation by rat IAPP can be rationalized by a model that postulates formation of an early helical intermediate during amyloid formation where the helical region is localized to the N-terminal region of IAPP. The model predicts that proline mutations in the putative helical region should lead to ineffective inhibitors as should mutations that alter the peptide−peptide interaction interface. We confirmed this by testing the ability of A13P and F15D point mutants of rat IAPP to inhibit amyloid formation by human IAPP. Both these mutants were noticeably less effective inhibitors than wild-type rat IAPP. The implications for inhibitor design are discussed.

Amyloid formation plays an important role in a broad range of human diseases, including Alzheimer's disease, Parkinson's disease, and type II diabetes (*1*−*3*). Islet amyloid polypeptide (IAPP),[1] also known as amylin, is a 37-residue polypeptide colocally produced with insulin and cosecreted by the pancreatic β-cells as a soluble monomer (*4*−*9*). IAPP is the major protein component of the pancreatic islet amyloid deposits often associated with type II diabetes (*4*, *5*). Formation of islet amyloid is believed to contribute to the pathology of the disease by promoting β-cell death, and there appears to be some correlation between the level of amyloid and the severity of the disease (*10*−*15*). Islet amyloid formation has also been proposed to be a potentially important complicating factor in islet cell transplantation (*16*−*18*).

The mature form of human IAPP has an amidated C-terminus and a disulfide bridge between residues Cys-2 and Cys-7 (Figure 1). Not all species form islet amyloid. In particular, human and non-human primates express a form of IAPP that can form amyloid fibrils, but rodents do not (*6*, *19*). The primary sequences of rodent and human IAPP are very similar aside from the region of residues 20−29. Mouse IAPP and rat IAPP have the same sequence and differ from the human protein at only six of 37 positions, five of which are located in the region of residues 20−29. There are three proline residues in this region of rat IAPP located at positions 25, 28, and 29, while human IAPP has none. Other differences are replacement of His-18 in human IAPP with Arg-18 in the rat sequence and substitution of Phe at position 23 and Ile at position 26 of the human sequence with Leu-23 and Val-26, respectively, in rat IAPP. The sequences of the human and rat polypeptides are shown in Figure 1.

The details of amyloid formation are still not well understood despite considerable effort, but recent experimental studies have led to the interesting suggestion that amyloid formation by human IAPP may proceed via a helical intermediate (*20*−*23*). Monomeric IAPP is a fluxional molecule that does not adopt a compact structure in isolation, but a rapidly growing body of experimental evidence clearly shows that certain regions of the polypeptide have a tendency to transiently sample partial helical conformations. A propensity for the preferential population of helical φ and ψ angles has been detected in NMR studies of both human and rat IAPP. The different studies reach slightly different conclusions about the exact boundaries of the partially helical region, but the broad consensus is that the region begins between residues 5 and 7 and extends to residues 20−22 or even further (*24*−*26*). Furthermore, it is well documented that helical

[†]This work was supported by National Institutes of Health Grant GM078114 to D.P.R.

*To whom correspondence should be addressed. Telephone: (631) 632-9547. Fax: (631) 632-7960. E-mail: draleigh@notes.cc.sunysb.edu.

[1]Abbreviations: AUC, analytical ultracentrifugation; CD, circular dichroism; IAPP, islet amyloid polypeptide; A13P-rIAPP, Ala-13 to Pro mutant of rat IAPP; F15D-rIAPP, Phe-15 to Asp mutant of rat IAPP; TEM, transmission electron microscopy; TFA, trifluoroacetic acid; T_{50}, time required to achieve 50% of the final thioflavin intensity in a kinetic experiment.

 Published on Web 12/22/2009

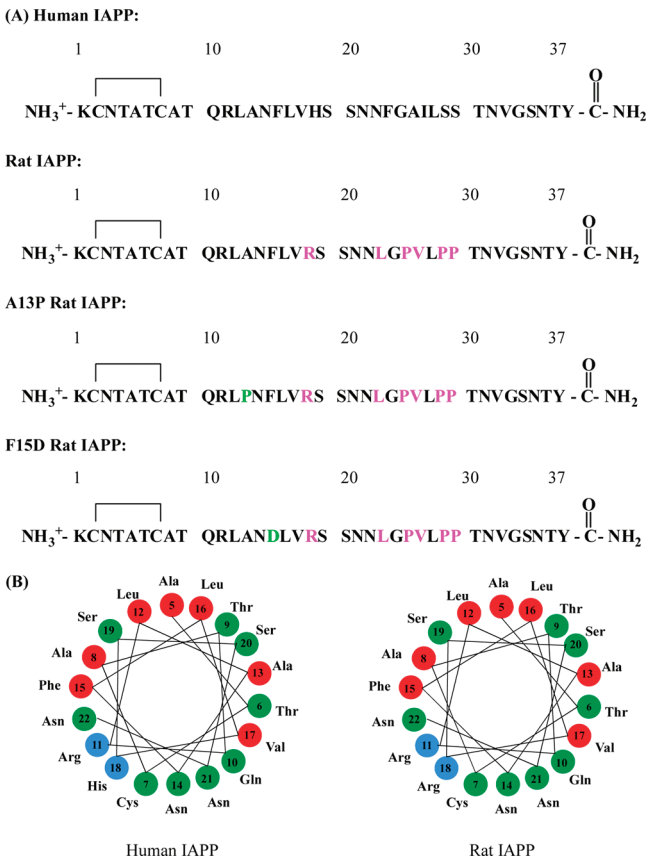

FIGURE 1: Comparison of human and rat IAPP. (A) Primary sequences of human IAPP, rat IAPP, and the A13P and F15D mutants of rat IAPP. All peptides have a disulfide bridge between Cys-2 and Cys-7 and have an amidated C-terminus. Residues that differ from that of the human peptide are colored pink. Residues in the mutants that differ from that of wild-type rat IAPP are colored light green. (B) Helical wheel representation of residues 5−22 of human and rat IAPP: red for nonpolar groups, green for polar, uncharged groups, and blue for basic groups.

structure can be promoted in the same region in IAPP by interactions with membranes or with other proteins or by the addition of low levels of helix-inducing cosolvents (*22*, *27*−*30*).

A model for helix-induced amyloid formation proposes that the initial oligomerization step is driven by the association of amphiphilic helices localized to a region starting between residues 5 and 7 and extending to around the vicinity of residues 20−24 (*20*−*23*). In this model, initial self-association is driven by the thermodynamic linkage between peptide association and the formation of the helical structure, a process which is well documented in many protein association domains (*31*, *32*). The association leads to a high local concentration of the C-terminal region of the polypeptide, and this segment is known to be extremely amyloidogenic (*33*). The model predicts that rat IAPP should be able to interact with the helical region of human IAPP but will inhibit amyloid formation since the C-terminal region of rat IAPP (residues 22−37) contains multiple proline substitutions that will inhibit the conversion to β-structure. The model further predicts that mutations that destabilize the propensity to form helical structure or disrupt the putative hydrophobic peptide−peptide interaction interface should lead to less effective inhibitors.

Here we test if rat IAPP inhibits amyloid formation by human IAPP and examine two mutants designed to test the proposed model. A13P rat IAPP, in which a single proline is substituted into the putative helical region, and a second mutant, F15D rat IAPP, designed to alter the potential peptide−peptide interaction interface were tested. Our studies confirm that rat IAPP is monomeric and lacks stable well-defined structure in aqueous solution. We show that rat IAPP is a moderate inhibitor of amyloid formation by human IAPP in vitro, and its behavior compares favorably to that of other reported inhibitors. Rat IAPP lengthens both the lag phase and the growth phase of the fibril formation pathway and decreases the final amount of amyloid fibrils in a dose-dependent manner. In contrast, the A13P rat IAPP and the F15D rat IAPP point mutants are noticeably less effective inhibitors.

EXPERIMENTAL PROCEDURES

Peptide Synthesis. Human IAPP, rat IAPP, A13P rat IAPP, and F15D rat IAPP were synthesized on a 0.25 mmol scale using an Applied Biosystems 433A peptide synthesizer, via 9-fluornylmethoxycarbonyl (Fmoc) chemistry. Solvents used were ACS grade. Fmoc-protected pseudoproline (oxazolidine) dipeptide derivatives were purchased from Novabiochem. All other reagents were purchased from Advanced Chemtech, PE Biosystems, Sigma, and Fisher Scientific. A 5-(4′-Fmoc-aminomethyl-3′,5-dimethoxyphenol)valeric acid (PAL-PEG) resin was used to form an amidated C-terminus. Standard Fmoc reaction cycles were used. The first residue attached to the resin, pseudoproline dipeptide derivatives, all β-branched residues, and all residues directly following a β-branched residue were double coupled (*34*). Peptides were cleaved from the resin using standard TFA methods.

Peptide Purification and Oxidation. Crude peptides were partially dissolved in 20% acetic acid (v/v), frozen in liquid nitrogen, and lyophilized. This procedure was repeated several times prior to purification to increase solubility. Disulfide bond formation was induced via oxidation by DMSO (*35*). The peptide was dissolved in 100% DMSO and allowed to stand at room temperature for a minimum of 5 h. The dry peptides were then redissolved in 30% acetic acid (v/v) and purified via reversed-phase HPLC, using a Vydac C18 preparative column (10 mm × 250 mm). A two-buffer system was used: buffer A consisting of 100% H_2O and 0.045% HCl (v/v) and buffer B consisting of 80% acetonitrile, 20% H_2O, and 0.045% (v/v) HCl. HCl was utilized as the ion pairing agent instead of TFA since TFA can influence the rate of aggregation. Purity was checked by HPLC using a Vydac C18 reversed-phase analytic column (4.6 mm × 250 mm) before each experiment. This is important because IAPP can undergo spontaneous deamidation. Peptides were analyzed by mass spectrometry using a Bruker MALDI-TOF MS instrument: oxidized rat IAPP, expected 3921.3, observed 3921.6; human IAPP, expected 3903.6, observed 3903.4; A13P rat IAPP, expected 3945.4, observed 3945.2; F15D rat IAPP, expected 3887.3, observed 3886.8.

Sample Preparation. A 1.6 mM peptide solution was prepared in 100% hexafluoro-2-propanol (HFIP) and stored at −20 °C. Amyloid formation was initiated by dilution of the stock solution as described below.

Thioflavin-T Binding Kinetic Experiments. Thioflavin-T binding assays were used to measure the development of structurally ordered fibrils over time. All fluorescence experiments were performed on an Applied Phototechnology fluorescence spectrophotometer using an excitation wavelength of 450 nm and an emission wavelength of 485 nm. The excitation and emission

slits were 5 nm. A 1.0 cm cuvette was used, and each point was averaged for 1 min. Solutions were prepared via dilution of a filtered stock peptide solution into 20 mM Tris-HCl buffer and thioflavin-T solution immediately before the measurement. A GHP Acrodisc 13 mm Syringe filter with a 0.45 μm GHP membrane was used. The conditions were as follows: 16 μM human IAPP, 25 μM thioflavin-T in 2% HFIP, 25 °C, and pH 7.4 for all experiments. All solutions were stirred during the experiments to maintain homogeneity. For seeding experiments, a fibril solution was prepared by dilution of 17 μL of a filtered stock solution into 20 mM Tris-HCl buffer to give a final concentration 16 μM. The solution was stirred for 80 min at 25 °C, a time that is longer than that required for formation of amyloid fibrils. Aliquots of this solution were used to seed other solutions. The solution was used within 8 h to ensure reproducibility of the seeding experiments. The concentration of the seeds was 1.6 μM in monomer units. The concentration of rat IAPP and rat IAPP mutants ranged from 16 to 160 μM depending upon the experiments.

Circular Dichroism (*CD*). CD spectra were recorded on an Applied Photophysics Chirascan circular dichroism spectrometer. For far-UV CD wavelength scans, the peptide solutions were prepared via dilution of the filtered stock peptide into 20 mM Tris-HCl buffer (pH 7.4). The final peptide concentrations for far-UV CD experiments were 16 μM in 2% HFIP. Spectra were recorded from 190 to 260 nm at 1 nm intervals in a quartz cuvette with a path length of 0.1 cm at 25 °C. CD experiments used the same stock solutions as the thioflavin-T fluorescence measurements.

Transmission Electron Microscopy (*TEM*). TEM was performed at the Life Science Microscopy Center at the State University of New York (Stony Brook, NY). TEM samples were prepared from the solutions used for the fluorescence measurements. Fifteen microliters of the peptide solution was removed at the end of the kinetic runs and placed on a carbon-coated Formvar 200 mesh copper grid for 1 min and then negatively stained with saturated uranyl acetate for 1 min.

Analytical Ultracentrifugation (*AUC*). Analytical ultracentrifugation was performed with a Beckman Optima XL-A analytical ultracentrifuge at 25 °C using rotor speeds of 38000 (24 h) and 48000 rpm (24 h). Apparent molecular masses were determined at initial peptide concentrations of 30, 60, and 90 μM rat IAPP in 20 mM Tris-HCl buffer (pH 7.4). Six-channel, 12 mm path length, charcoal-filled Epon cells with quartz windows were used. The absorbance was measured at 280 nm, and 10 scans were averaged. The partial specific volume (0.7278 mL/g) and solution density (1.003 g/L) were calculated with SEDNTERP. Hetero-Analysis from the Analytical Ultracentrifugation Facility at the University of Connecticut was used for data analysis.

Gel Filtration. Gel filtration measurements were performed using an AKTA purifier 10 FPLC instrument (GE Healthcare) at 4 °C and a Superdex 75 10/300 GL column. The flow rate was set to 0.5 mL/min. Peptides were loaded at a concentration of 160 μM in 20 mM Tris-HCl buffer (pH 7.4). Twenty millimolar Tris-HCl buffer (pH 7.4) with 0.15 M NaCl was used as the buffer system. Wild-type rat IAPP, which is monomeric under these conditions, was used as control at the same concentration.

RESULTS AND DISCUSSION

Rat IAPP Is Monomeric in Aqueous Solution. Rat IAPP is well known not to form amyloid (*19*). The association state of rat IAPP was examined using analytical ultracentrifugation (AUC) because self-association, even in the absence of amyloid formation, could lead to apparent effects on the formation of human IAPP oligomers and fibrils. AUC experiments confirmed that rat IAPP is monomeric under the conditions of these studies (Supporting Information). The AUC data were fit well by an ideal single-species model with a molecular weight within 5% of the monomer molecular weight. The average apparent experimental molecular weight determined from multiple experiments with rat IAPP over the concentration range of 30−90 μM is 4102.0, and the expected mass is 3921.3. CD experiments confirmed that rat IAPP does not adopt well-ordered structure under the conditions of our studies (Supporting Information).

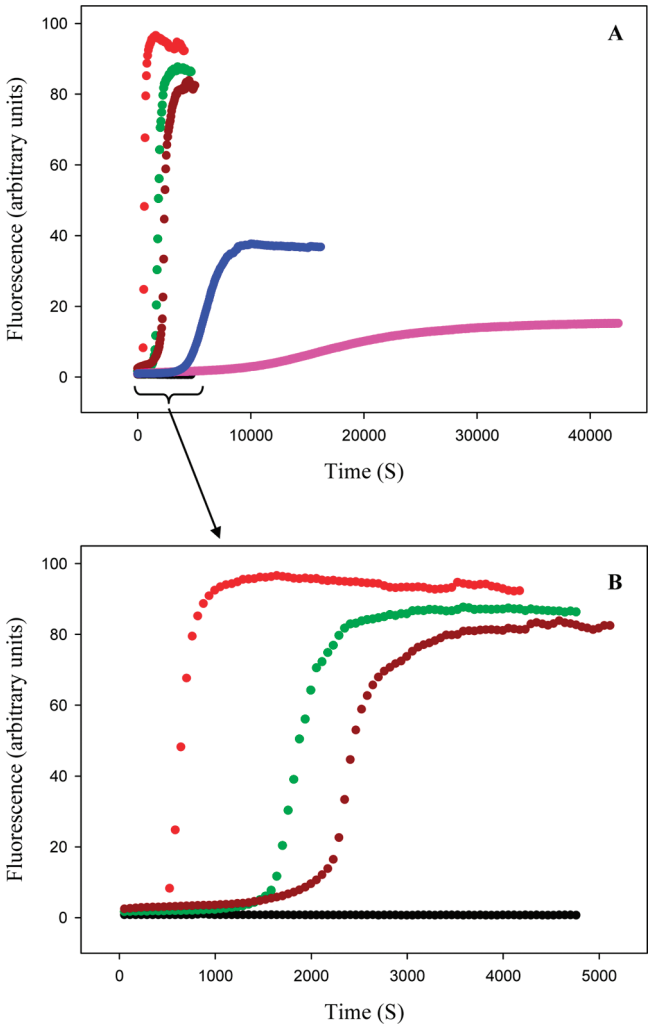

FIGURE 2: Rat IAPP inhibits amyloid formation by human IAPP. (A) Results of fluorescence-monitored thioflavin-T kinetic experiments are shown: red for human IAPP, black for rat IAPP, green for rat IAPP and human IAPP at a 1:1 ratio, dark red for rat IAPP and human IAPP at a 2:1 ratio, blue for rat IAPP and human IAPP at a 5:1 ratio, and pink for rat IAPP and human IAPP at a 10:1 ratio. (B) Expansion of the first 5000 s of panel A for the pure human IAPP sample and the 1:1 and 2:1 mixtures of rat IAPP and human IAPP, as well as the sample of pure rat IAPP. All experiments were performed at 25 °C and pH 7.4 in 16 μM IAPP, 20 mM Tris-HCl, and 25 μM thioflavin-T in 2% HFIP (v/v) with constant stirring. The concentration of rat IAPP ranged from 16 μM for the sample of pure rat IAPP and for the 1:1 sample to 160 μM for the 10:1 sample.

Rat IAPP Inhibits Amyloid Formation by Human IAPP in a Dose-Dependent Manner. The ability of human IAPP and rat IAPP to form amyloid fibrils was first tested using

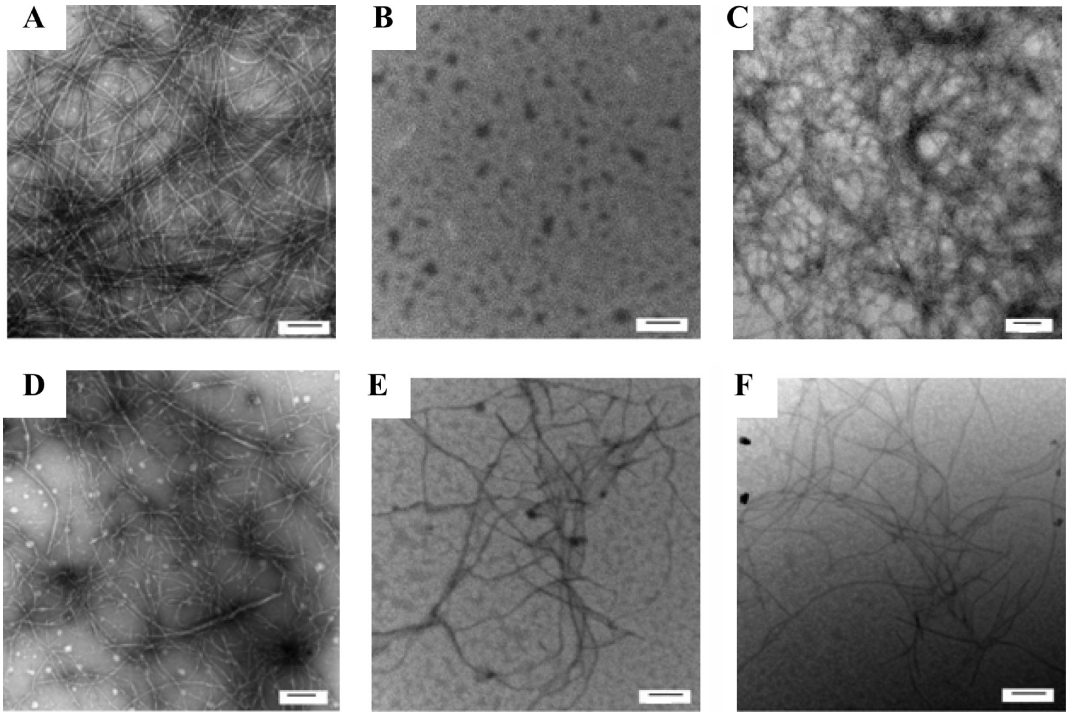

FIGURE 3: Transmission electron microscopy confirms that rat IAPP inhibits amyloid formation by human IAPP. Samples were removed at the end of the kinetic reactions shown in Figure 2, and TEM images recorded: (A) human IAPP, (B) rat IAPP, (C) 1:1 mixture of rat IAPP and human IAPP, (D) 2:1 mixture of rat IAPP and human IAPP, (E) 5:1 mixture of rat IAPP and human IAPP, and (F) 10:1 mixture of rat IAPP and human IAPP. The scale bar represents 100 nm.

thioflavin-T binding assays. The fluorescence-detected thioflavin-T binding assay is the standard method used to monitor the time course of fibril formation (*36*). The dye experiences a significant increase in quantum yield upon binding to amyloid fibrils. The exact mode of binding is not known, but the dye is believed to bind to grooves formed on the surface of amyloid fibrils by aligned rows of side chains. The data collected for human IAPP show a typical IAPP fibrillization process with a lag phase of ~10 min followed by a growth phase and a final plateau in which fibrils are in equilibrium with soluble IAPP (Figure 2). TEM images recorded at the end point of the reaction display the classic features of human IAPP amyloid fibrils (Figure 3A). However, the results of the rat IAPP experiment are strikingly different. As expected, on the basis of past studies, no significant change in thioflavin-T fluorescence is observed over the entire time course of the reaction, and TEM images of the end product reveal that no fibrils was formed (Figure 3B). CD spectra recorded at the end of the kinetic runs show that the human IAPP sample is rich in β-structure, while the rat peptide is not (Supporting Information).

Important early work used thioflavin-T assays to show that rat IAPP lengthened the lag phase of human IAPP and reduced the final fluorescence intensity; however, a quantitative analysis of the progress curves has not been reported, nor was the final morphology of the products examined (*37*). The ability of rat IAPP to inhibit amyloid formation by human IAPP was tested at various ratios of rat to human IAPP. A 1:1 mixture of rat and human IAPP exhibits a lag phase that is 2.5 times longer than that observed for human IAPP alone, and a small but reproducible decrease in the final thioflavin-T fluorescence intensity is detected (Figure 2). More dramatic effects are observed at higher ratios of rat IAPP to human IAPP. The lag phase is increased by a factor of approximately 3.3 for the 2:1 mixture of rat and human IAPP relative to the uninhibited human IAPP control. The lag phase increases monotonically with an increasing rat IAPP concentration and is 10-fold longer for the 5:1 rat IAPP/human IAPP sample and 22-fold longer for the 10:1 rat IAPP/human IAPP sample relative to the value observed in the absence of rat IAPP. The final thioflavin fluorescence is also reduced in a dose-dependent manner. The final fluorescence intensity is often used as a measure of the amount of amyloid formed; however, the intensity is also affected by a variety of factors, and considerable caution should be applied before interpreting thioflavin-T fluorescence intensity as a direct readout of the amount of amyloid. The final fluorescence intensity of the 5:1 human IAPP/rat IAPP mixture decreased by 67% relative to that of the sample of pure human IAPP and is reduced by 85% in the 10:1 rat IAPP/human IAPP sample. These results are not due to a change in the amount of human IAPP present since all samples contained the same amount of human IAPP. The rat peptide alone has no effect on the observable thioflavin-T fluorescence at all concentrations examined (16−160 μM).

Thioflavin-T assays can give false positives in inhibitor assays since a number of factors can lead to a loss of thioflavin-T fluorescence besides the direct inhibition of amyloid formation (*38*). Thus, it is critical to assay any potential inhibitors by an independent method. Aliquots of each reaction mixture were collected at a time point after the final fluorescence had reached the steady-state value, and TEM images recorded. Amyloid fibrils were present in the 1:1 rat IAPP/human IAPP mixture; however, fewer fibrils were detected in the other mixtures, and the morphology was clearly different. In particular, the TEM images recorded for the 5:1 and 10:1 rat IAPP/human IAPP mixtures showed significantly thinner fibrils (Figure 3C−F).

Examination of the kinetic curves displayed in Figure 2 indicates that rat IAPP alters both the lag time and the growth phase. Figure 4A displays a plot of the length of the lag phase, which is defined here as the time required to achieve 10% of the final fluorescence intensity, and the T_{50} times. T_{50} is defined as the

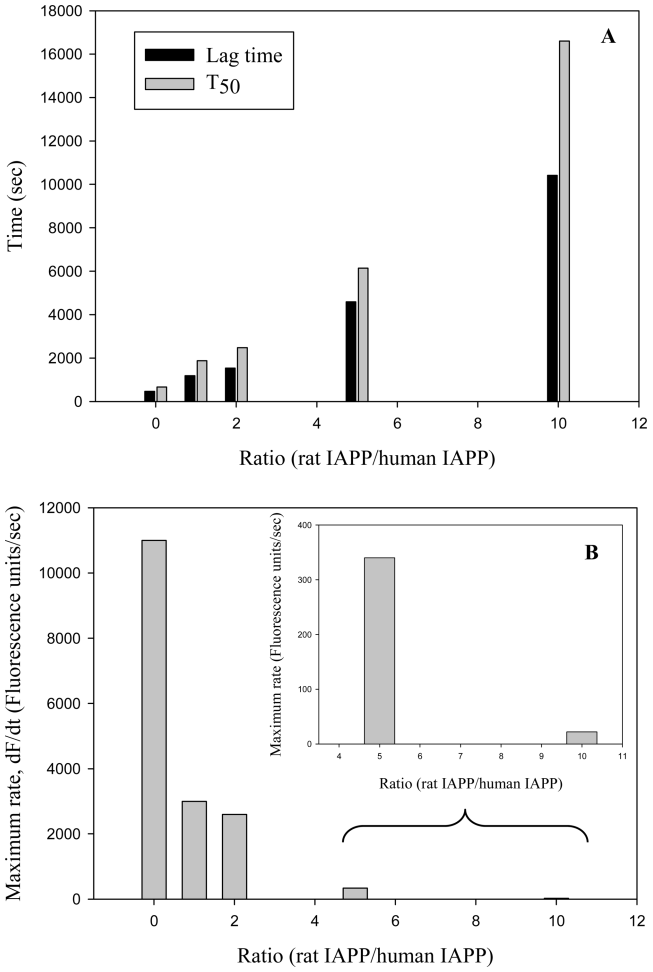

FIGURE 4: Effect of rat IAPP on the lag phase and growth rate of human IAPP amyloid formation. (A) Rat IAPP lengthens the lag time for amyloid formation by human IAPP. The bar graph compares the experimental T_{50} time and lag time, for different ratios of rat to human IAPP ranging from 0 (pure human IAPP) to a 10-fold excess of rat IAPP (16 μM human IAPP and 160 μM rat IAPP). The lag time is defined as the time required to reach 10% of the final thioflavin-T fluorescence intensity. (B) Rat IAPP decreases the maximum rate of growth. The bar graph compares the maximum growth rate dF/dt for different ratios of rat to human IAPP ranging from 0 (pure human IAPP) to a 10-fold excess of rat IAPP. The inset shows an expansion of the data for the 5:1 and 10:1 ratios.

time needed to reach 50% of the final fluorescence intensity and includes contributions from both the lag phase and the growth phase. A more quantitative measure of the effects upon the growth phase can be obtained via calculation of the apparent maximum rate, which is the apparent rate at T_{50}. The calculation is easily performed by numerical differentiation of the kinetic progress curve. The kinetic curves were fit to an empirical function that described a sigmoidal curve, and the resulting parameters were used to calculate a plot of the derivative $dF(t)/dt$, where $F(t)$ represents the fluorescence intensity, versus time (Supporting Information). This plot gives T_{50} and the maximum rate, i.e., dF/dt at $t = T_{50}$. As the amount of rat IAPP increases, the rate at T_{50} decreases (Figure 4B). These results quantitatively confirm that rat IAPP inhibits amyloid formation by lengthening both the lag phase and the growth phase.

Demonstration of an Interaction between Rat and Human IAPP. Surface plasmon resonance has been used to demonstrate an interaction between rat IAPP and surface-immobilized biotinylated human IAPP (*39*). To test for a direct

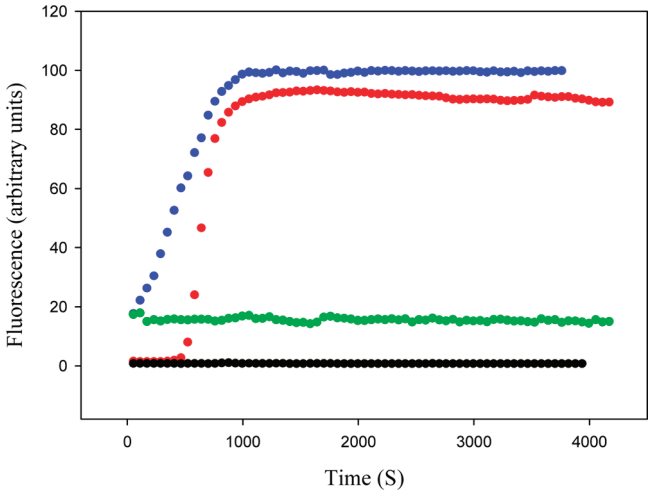

FIGURE 5: Human IAPP amyloid fibrils do not seed amyloid formation by rat IAPP. Fluorescence-monitored thioflavin-T kinetic experiments are shown: red for unseeded human IAPP, black for unseeded rat IAPP, blue for human IAPP seeded by human IAPP fibrils, and green for rat IAPP seeded by human IAPP fibrils. Experiments were performed at 25 °C and pH 7.4 in 20 mM Tris-HCl and 25 μM thioflavin-T in 2% (v/v) HFIP with constant stirring. The peptide concentration was 16 μM for human IAPP and 16 μM for rat IAPP. Human IAPP seeds, when added, were present at a monomer concentration of 1.6 μM.

interaction between rat and human IAPP in solution, far-UV CD spectroscopy was employed. Spectra were recorded when the final fluorescence intensity reached the plateau value at the same time point that the TEM images were recorded. The CD spectrum of human IAPP indicated significant amounts of β-sheet structure, while the spectrum of rat IAPP was consistent with a flexible largely unstructured polypeptide (Supporting Information). Spectra were also recorded for the various mixtures of human and rat IAPP and were compared to the spectrum expected for a noninteracting mixture of the two peptides. The expected spectrum of a non-interacting mixture is easily calculated as the appropriately weighted sum of the spectrum of the sample of pure human IAPP and the spectrum of the sample of pure rat IAPP. Any differences between the observed and calculated spectra provide direct evidence of an interaction between the two peptides. The experimental spectra of the mixtures clearly differ from spectra calculated for a noninteracting mixture of the two peptides (Supporting Information).

Human IAPP Fibrils Do Not Seed Amyloid Formation by Rat IAPP. A characteristic feature of amyloid formation is that the reaction can be seeded via addition of small amounts of preformed amyloid fibrils to a soluble sample of protein. The seeds act as templates for rapid fibril growth and lead to the bypassing of the lag phase. Having demonstrated the interaction of rat IAPP with human IAPP, we next sought to determine if rat IAPP can bind to seeds made from human IAPP fibrils; thus, we are asking whether human IAPP can efficiently seed fibril formation by rat IAPP. Human IAPP fibrils formed at the end of a kinetic run with pure human IAPP were used to seed a solution of rat IAPP at a ratio of 10% seeds. Kinetic curves presented in Figure 5 demonstrate that mature human IAPP fibrils are not capable of seeding fibril formation by rat IAPP under these conditions. The fluorescence intensity of the mixture of rat IAPP with the human IAPP seeds is slightly higher than that of the rat IAPP reaction alone, but this is due to the fact that human amyloid fibril seeds bind to thioflavin-T. The critical

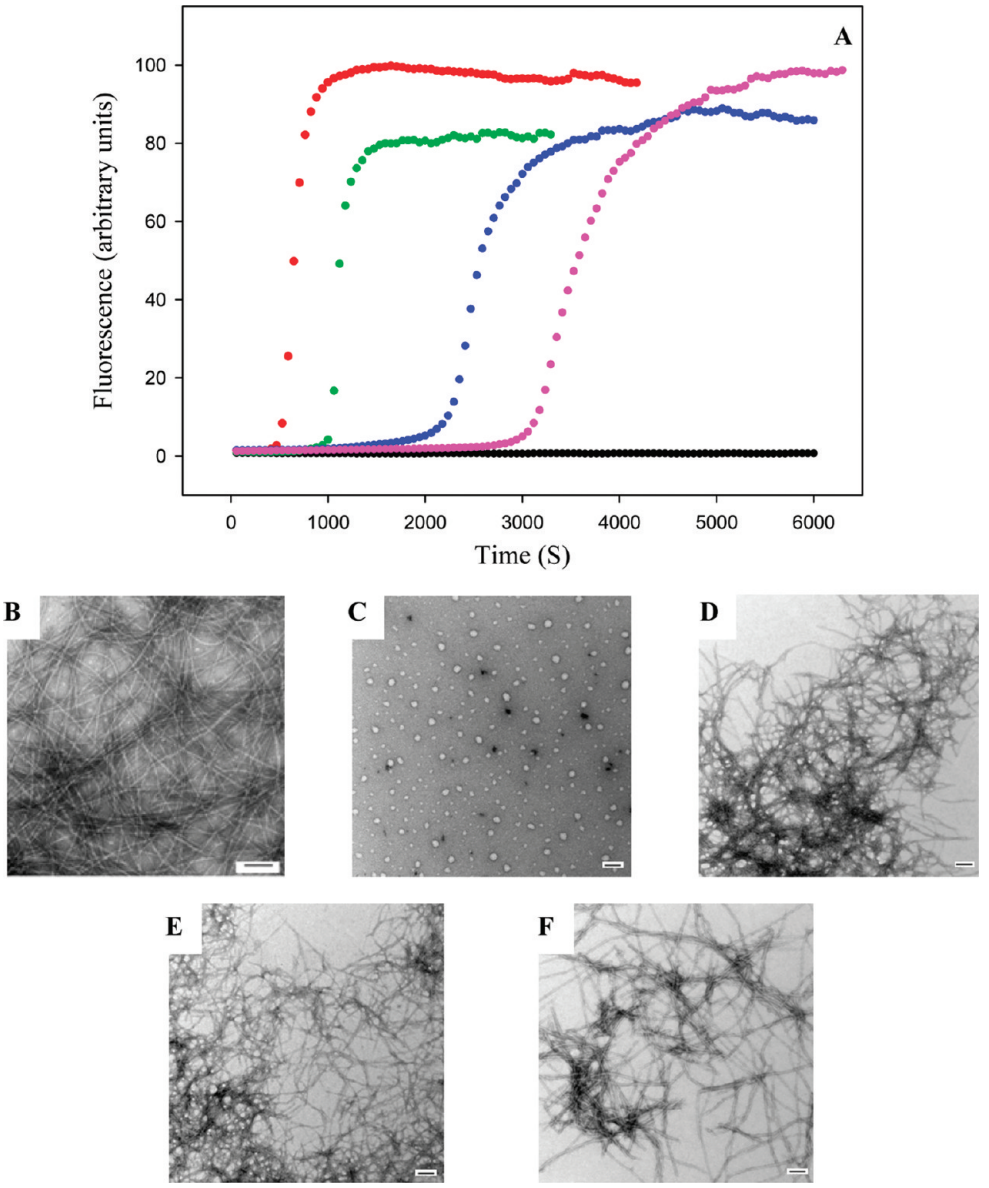

FIGURE 6: The A13P mutant of rat IAPP is a less effective inhibitor of amyloid formation than wild-type rat IAPP. (A) Results of fluorescence-monitored thioflavin-T kinetic experiments are shown: red for human IAPP, black for A13P-rat IAPP, green for A13P-rat IAPP and human IAPP at a 1:1 ratio, blue for A13P-rat IAPP and human IAPP at a 5:1 ratio, and pink for A13P-rat IAPP and human IAPP at a 10:1 ratio. All experiments were performed at 25 °C and pH 7.4 in 16 μM IAPP, 20 mM Tris-HCl, and 25 μM thioflavin-T in 2% (v/v) HFIP with constant stirring. The concentration of A13P-rat IAPP ranged from 16 μM for the sample of pure A13P-rat IAPP and for the 1:1 sample to 160 μM for the 10:1 sample. (B−F) Transmission electron microscopy confirms that A13P-rat IAPP is a less effective inhibitor. Samples were removed at the end of the kinetic reactions, and TEM images were recorded: (B) human IAPP, (C) A13P-rat IAPP, (D) 1:1 A13P-rat IAPP/human IAPP mixture, (E) 5:1 A13P-rat IAPP/human IAPP mixture, and (F) 10:1 A13P-rat IAPP/human IAPP mixture.

observation is that no significant change in thioflavin-T fluorescence is observed over the time course of the reaction. In contrast, addition of the human IAPP seeds to the human IAPP reaction abolished the lag phase as expected (Figure 5).

Point Mutations That Disrupt the Putative Helical Region of Rat IAPP or Target Its Ability To Interact with Human IAPP Lead to Much Less Effective Inhibitors. Our model for the mode of inhibition of human IAPP amyloid formation by rat IAPP proposes that the polypeptides interact via their respective N-terminal regions and suggests that these interactions are mediated by helical association. The model predicts that mutations that reduce the propensity of rat IAPP to sample helical conformations should lead to a less effective inhibitor. Consequently, we prepared a point mutant of rat IAPP, A13P-rat IAPP, in which Ala-13, a residue near the center of the putative helical region, is replaced with Pro. The substitution will significantly reduce the propensity of the polypeptide to sample helical conformations. As expected, the mutant is monomeric (Supporting Information), and CD indicates that it does not adopt a well-structured conformation.

The mutant is less effective at inhibiting amyloid formation by human IAPP than is the rat polypeptide. Figure 6 displays the results of a set of thioflavin-T fluorescence-monitored kinetic experiments conducted at various ratios of A13P-rat IAPP to human IAPP. The time to reach 50% of the final fluorescence intensity, T_{50}, is 5.3 times longer for the 10:1 mixture of A13P-rat IAPP and human IAPP than for a sample of pure human IAPP. In contrast, a 10-fold excess of wild-type rat IAPP increases the T_{50} value by ~25-fold; thus, by this criterion, the mutant is 4.6 times less effective. The A13P-rat IAPP mutant has no significant

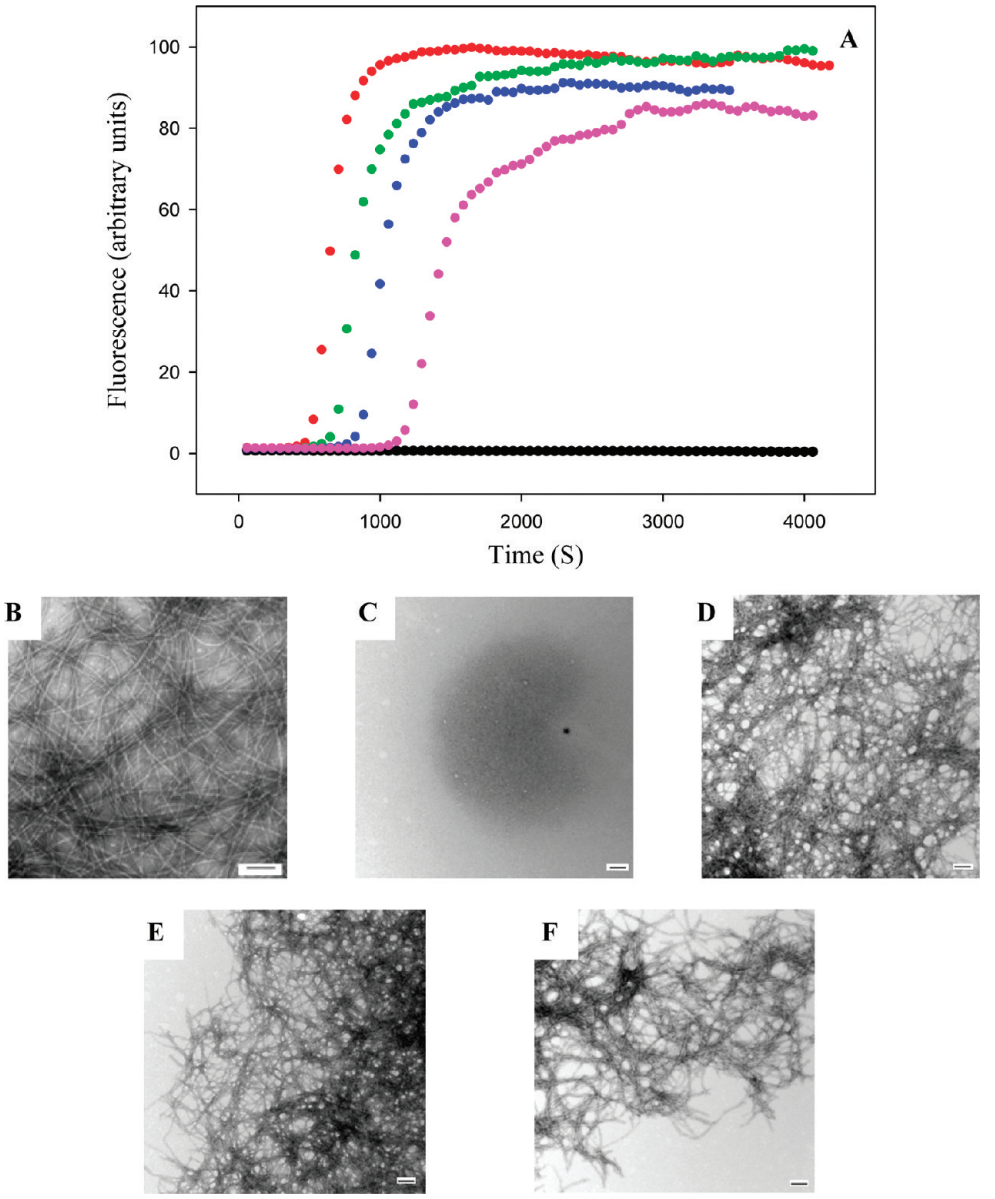

FIGURE 7: The F15D mutant of rat IAPP is a less effective inhibitor of amyloid formation than wild-type rat IAPP. (A) Results of fluorescence-monitored thioflavin-T kinetic experiments are shown: red for human IAPP, black for F15D-rat IAPP, green for F15D-rat IAPP and human IAPP at a 1:1 ratio, blue for F15D-rat IAPP and human IAPP at a 5:1 ratio, and pink for F15D-rat IAPP and human IAPP at a 10:1 ratio. All experiments were performed at 25 °C and pH 7.4 in 16 μM IAPP, 20 mM Tris-HCl, and 25 μM thioflavin-T in 2% (v/v) HFIP with constant stirring. The concentration of F15D-rat IAPP ranged from 16 μM for the sample of pure F15D rat IAPP and for the 1:1 sample to 160 μM for the 10:1 sample. (B−F) Transmission electron microscopy confirms that F15D-rat IAPP is a less effective inhibitor. Samples were removed at the end of the kinetic reactions, and TEM images were recorded: (B) human IAPP, (C) F15D-rat IAPP, (D) 1:1 F15D-rat IAPP/human IAPP mixture, (E) 5:1 F15D-rat IAPP/human IAPP mixture, and (F) 10:1 F15D-rat IAPP/human IAPP mixture.

effect on the final thioflavin-T fluorescence intensity even when added at a 10-fold excess, while a 10-fold excess of the wild-type rat polypeptide reduces the final thioflavin-T fluorescence by 85%. The mutant is also much less effective at inhibiting the growth rate. The maximum rate in the presence of a 10-fold excess of the A13P mutant is more than 55 times larger than the maximum rate observed in the presence of a 10-fold excess of wild-type rat IAPP. The mutant is also less effective than the wild-type rat polypeptide when added at a 5:1 or 1:1 ratio. The kinetic data are summarized in Table 1. TEM studies confirm the results of the kinetic experiments. TEM images of samples collected at the end of the respective kinetic runs are included in Figure 6. Amyloid fibers are observed even for the experiment conducted with a 10-fold excess of the mutant polypeptide, although they appear somewhat less numerous than those observed in the presence of smaller amounts of the A13P-rat IAPP mutant. Both the 1:1 and 5:1 samples exhibit dense mats of fibrils.

The proline mutant will weaken the ability of the rat peptide to adopt helical structure (Supporting Information). A more subtle mutation might target the putative interaction interface while not completely disrupting helical structure. We choose to target Phe-15. This residue has been proposed to play an important role in the initial events of human IAPP self-association and in insulin IAPP interactions (*22*, *40*). The latter is particularly interesting in the context of inhibitor design since insulin is one of the most potent inhibitors of IAPP amyloid formation known (*39*−*42*). We replace Phe-15 with Asp. An Asp substitution was chosen because the mutation replaces a large residue with a small one and introduces a charge into what would be a hydrophobic

Table 1: Comparison of Kinetic Parameters for Human IAPP Amyloid Formation in the Presence and Absence of Rat IAPP and Mutants of Rat IAPP

	lag time (s)	T_{50} (s)	maximum rate (fluorescence units/s)
pure human IAPP	470	670	11000
1:1 rat IAPP:human IAPP	1180	1870	3000
2:1 rat IAPP:human IAPP	1530	2480	2600
5:1 rat IAPP:human IAPP	4590	6140	340
10:1 rat IAPP:human IAPP	10410	16600	22.0
pure human IAPP	470	670	11000
1:1 A13P-rat IAPP:human IAPP	1010	1090	10642
5:1 A13P-rat IAPP:human IAPP	2180	2400	2084
10:1 A13P-rat IAPP:human IAPP	3130	3600	1260
pure human IAPP	470	670	11000
1:1 F15D-rat IAPP:human IAPP	700	830	6773
5:1 F15D-rat IAPP:human IAPP	880	1010	6319
10:1 F15D-rat IAPP:human IAPP	1200	1400	3402

interface. Thioflavin-T fluorescence assays demonstrate that the F15D-rat IAPP is a much less effective inhibitor than wild-type rat IAPP (Figure 7). When added in a 10-fold excess, the F15D-rat IAPP mutant increases the T_{50} value relative to that of pure human IAPP by a little more than a factor of 2 compared to the 25-fold effect observed with the wild-type rat IAPP. The mutant has a modest effect on the final thioflavin-T fluorescence intensity with a 10-fold excess of mutant inhibitor leading to an only 15% decrease relative to the uninhibited value. The effect on the growth rate is also modest, and a 10-fold excess of mutant inhibitor reduces the maximum rate by a factor of 3 relative to the value measured in the absence of the inhibitor, while a 10-fold excess of the wild-type rat polypeptide decreases the maximum rate by a factor of more than 55. The mutant is also less effective than the wild-type inhibitor when added at a 5-fold excess or at a 1:1 ratio (Table 1). TEM images of the final reaction products are included in Figure 7. Dense collections of amyloid fibers are observed for all samples, including the one in which the mutant inhibitor is present in 10-fold excess relative to human IAPP.

Both the A13P and F15D mutants have a significant effect on the ability of rat IAPP to inhibit amyloid formation by human IAPP. It is formally possible that the effects could be indirect in the sense that the mutants might have the unanticipated effect of promoting self-association of the inhibitor, thereby reducing the amount of inhibitor actually available to interact with human IAPP. This is an unlikely scenario, but it is important to test for it. Consequently, we examined the properties of the mutants at the highest concentration used, 160 μM. Gel filtration (Supporting Information) confirms that both peptides are monomeric, while CD indicates that they do not adopt well-ordered structure. Neither mutant binds thioflavin even at the highest concentration.

CONCLUSIONS

The data presented here demonstrate that rat IAPP inhibits amyloid formation by human IAPP, lengthening both the lag phase and the growth phase in a dose-dependent manner and altering the morphology of the fibrils that are formed, as well as reducing the final thioflavin-T fluorescence intensity. The rat peptide is a less effective inhibitor than some other variants of full-length human IAPP that contain fewer substitutions (*43*, *44*). The potential mode of action of those peptides has not been discussed in the literature, but interestingly, they contain either a single proline mutation in the region of residues 20−29 or double *N*-methyl substitutions in the same region. Thus, they likely act in a fashion very similar to that of rat IAPP. The simplest possible rationalization of the reduced potency of rat IAPP relative to these variants is that the multiple substitutions in rat IAPP lead to a weaker interaction with human IAPP. Irrespective of the mechanistic details, the combination of a motif that can recognize pre-β-sheet species formed by human IAPP together with a segment that prevents β-sheet formation is likely to be a broadly applicable approach to the development of inhibitors of human IAPP amyloid formation. Although rat IAPP is less effective than some full-length variants of human IAPP, it is as effective at inhibiting amyloid formation as a number of small molecules and peptide-based inhibitors (*45*−*48*).

The behavior of the mutant rat peptides is consistent with our proposed model of rat IAPP's ability to inhibit amyloid formation. The model postulates that rat IAPP takes part in early oligomerization involving residues in the putative helical region. The proline substitution is located in the middle of that segment, and proline is the most helix destabilizing of the coded amino acids. Thus, the A13P substitution should lead to less effective protein−protein interactions. Of course, the proline mutant might also exert some of its effects by directly disrupting protein−protein interaction surfaces as well as by reducing helical propensity. The F15D mutant is far more conservative in terms of helical propensity but is nonconservative in that it replaces a large hydrophobic residue with a small charged residue. F15 has been proposed to be involved in the early oligomerization steps of amyloid formation (*22*, *40*) by participating in peptide−peptide interactions. Our conceptual model proposes that rat IAPP inhibits amyloid formation by human IAPP because it substitutes for human IAPP in these initial steps. The model predicts that mutations that drastically alter the interaction interface should affect the ability of rat IAPP to act as an inhibitor. This is precisely what is observed with the F15D-rat IAPP mutant. Interestingly, the F15D mutant appears to have a somewhat more pronounced effect on the ability of rat IAPP to act as an amyloid inhibitor than does the A13P mutant. This may indicate that alteration of the hydrophobic nature of the putative peptide−peptide interface is more important than reducing the helical propensity. Irrespective of the mechanistic details, the behavior of the two mutants is consistent with the proposed model.

The ability of rat IAPP has interesting implications for transgenic mouse models of islet amyloid, as has been previously noted (*37*, *49*). A number of mouse and rat models have been developed which express human IAPP for the investigation of the adverse effects of human IAPP amyloid formation (*14*, *37*, *50*−*58*). However, if mouse IAPP inhibits amyloid formation by human IAPP in vivo as well as in vitro, then the results of transgenic mouse experiments that involve mouse models that are heterozygous for mouse and human IAPP may be misleading.

ACKNOWLEDGMENT

We thank Professor Martin Zanni, Dr. Chris Middleton, and members of the Raleigh group for helpful discussions.

SUPPORTING INFORMATION AVAILABLE

Results of the sedimentation equilibrium studies of rat IAPP, plots of the derivative of the thioflavin-T fluorescence versus time, experimental CD spectra and calculated CD spectra of rat and human IAPP as well as 1:1, 2:1, and 5:1 mixtures of rat and

human IAPP, results of gel filtration experiments conducted on A13P-rat IAPP and F15D-rat IAPP, and an AGADIR analysis of the helical propensity of rat IAPP, A13P-rat IAPP, and F15D-rat IAPP. This material is available free of charge via the Internet at http://pubs.acs.org.

REFERENCES

1. Chiti, F., and Dobson, C. M. (2006) Protein misfolding, functional amyloid, and human disease. *Annu. Rev. Biochem. 75*, 333–366.
2. Sipe, J. D. (1994) Amyloidosis. *Crit. Rev. Clin. Lab. Sci. 31*, 325–354.
3. Selkoe, D. J. (2004) Cell biology of protein misfolding: The examples of Alzheimer's and Parkinson's diseases. *Nat. Cell Biol. 6*, 1054–1061.
4. Westermark, P., Wernstedt, C., Wilander, E., Hayden, D. W., Obrien, T. D., and Johnson, K. H. (1987) Amyloid fibrils in human insulinoma and islets of langerhans of the diabetic cat are derived from a neuropeptide-like protein also present in normal islet cells. *Proc. Natl. Acad. Sci. U.S.A. 84*, 3881–3885.
5. Cooper, G. J. S., Willis, A. C., Clark, A., Turner, R. C., Sim, R. B., and Reid, K. B. M. (1987) Purification and characterization of a peptide from amyloid-rich pancreases of type-2 diabetic-patients. *Proc. Natl. Acad. Sci. U.S.A. 84*, 8628–8632.
6. Cooper, G. J. S. (1994) Amylin compared with calcitonin-gene-related peptide: Structure, biology, and relevance to metabolic disease. *Endocr. Rev. 15*, 163–201.
7. Kahn, S. E., Dalessio, D. A., Schwartz, M. W., Fujimoto, W. Y., Ensinck, J. W., Taborsky, G. J., and Porte, D. (1990) Evidence of cosecretion of islet amyloid polypeptide and insulin by β-cells. *Diabetes 39*, 634–638.
8. Marzban, L., Trigo-Gonzales, G., Zhu, X. R., Rhodes, C. J., Halban, P. A., Steiner, D. F., and Verchere, C. B. (2004) Role of β-cell prohormone convertase (PC) 1/3 in processing of pro-islet antyloid polypeptide. *Diabetes 53*, 141–148.
9. Sanke, T., Bell, G. I., Sample, C., Rubenstein, A. H., and Steiner, D. F. (1988) An islet amyloid peptide is derived from an 89-amino acid precursor by proteolytic processing. *J. Biol. Chem. 263*, 17243–17246.
10. Lorenzo, A., Razzaboni, B., Weir, G. C., and Yankner, B. A. (1994) Pancreatic-islet cell toxicity of amylin associated with type-2 diabetes-mellitus. *Nature 368*, 756–760.
11. Clark, A., Lewis, C. E., Willis, A. C., Cooper, G. J. S., Morris, J. F., Reid, K. B. M., and Turner, R. C. (1987) Islet amyloid formed from diabetes-associated peptide may be pathogenic in type-2 diabetes. *Lancet 2*, 231–234.
12. Hull, R. L., Westermark, G. T., Westermark, P., and Kahn, S. E. (2004) Islet amyloid: A critical entity in the pathogenesis of type 2 diabetes. *J. Clin. Endocr. Metab. 89*, 3629–3643.
13. Clark, A., Wells, C. A., Buley, I. D., Cruickshank, J. K., Vanhegan, R. I., Matthews, D. R., Cooper, G. J. S., Holman, R. R., and Turner, R. C. (1988) Islet amyloid, increased α-cells, reduced β-cells and exocrine fibrosis: Quantitative changes in the pancreas in type-2 diabetes. *Diabetes Res. 9*, 151–159.
14. Hayden, M. R., Karuparthi, P. R., Manrique, C. M., Lastra, G., Habibi, J., and Sowers, J. R. (2007) Longitudinal ultrastructure study of islet amyloid in the HIP rat model of type 2 diabetes mellitus. *Exp. Biol. Med. 232*, 772–779.
15. Kahn, S. E., Andrikopoulos, S., and Verchere, C. B. (1999) Islet amyloid: A long-recognized but underappreciated pathological feature of type 2 diabetes. *Diabetes 48*, 241–253.
16. Westermark, G. T., Westermark, P., Berne, C., Korsgren, O., and Transpla, N. N. C. I. (2008) Widespread amyloid deposition in transplanted human pancreatic islets. *N. Engl. J. Med. 359*, 977–979.
17. Westermark, G. T., Westermark, P., Nordin, A., Tornelius, E., and Andersson, A. (2003) Formation of amyloid in human pancreatic islets transplanted to the liver and spleen of nude mice. *Upsala J. Med. Sci. 108*, 193–203.
18. Udayasankar, J., Kodama, K., Hull, R. L., Zraika, S., Aston-Mourney, K., Subramanian, S. L., Tong, J., Faulenbach, M. V., Vidal, J., and Kahn, S. E. (2009) Amyloid formation results in recurrence of hyperglycaemia following transplantation of human IAPP transgenic mouse islets. *Diabetologia 52*, 145–153.
19. Westermark, P., Engstrom, U., Johnson, K. H., Westermark, G. T., and Betsholtz, C. (1990) Islet amyloid polypeptide: Pinpointing amino-acid-residues linked to amyloid fibril formation. *Proc. Natl. Acad. Sci. U.S.A. 87*, 5036–5040.
20. Abedini, A., and Raleigh, D. P. (2009) A role for helical intermediates in amyloid formation by natively unfolded polypeptides? *Phys. Biol. 6*, 15005.
21. Abedini, A., and Raleigh, D. P. (2009) A critical assessment of the role of helical intermediates in amyloid formation by natively unfolded proteins and polypeptides. *Protein Eng., Des. Sel. 22*, 453–459.
22. Wiltzius, J. J. W., Sievers, S. A., Sawaya, M. R., and Eisenberg, D. (2009) Atomic structures of IAPP (amylin) fusions suggest a mechanism for fibrillation and the role of insulin in the process. *Protein Sci. 18*, 1521–1530.
23. Williamson, J. A., Loria, J. P., and Miranker, A. D. (2009) Helix stabilization precedes aqueous and bilayer-catalyzed fiber formation in islet amyloid polypeptide. *J. Mol. Biol. 393*, 383–396.
24. Williamson, J. A., and Miranker, A. D. (2007) Direct detection of transient α-helical states in islet amyloid polypeptide. *Protein Sci. 16*, 110–117.
25. Wei, L., Jiang, P., Yau, Y. H., Summer, H., Shochat, S. G., Mu, Y. G., and Pervushin, K. (2009) Residual structure in islet amyloid polypeptide mediates its interactions with soluble insulin. *Biochemistry 48*, 2368–2376.
26. Yonemoto, I. T., Kroon, G. J. A., Dyson, H. J., Balch, W. E., and Kelly, J. W. (2008) Amylin proprotein processing generates progressively more amyloidogenic peptides that initially sample the helical state. *Biochemistry 47*, 9900–9910.
27. Knight, J. D., Hebda, J. A., and Miranker, A. D. (2006) Conserved and cooperative assembly of membrane-bound α-helical states of islet amyloid polypeptide. *Biochemistry 45*, 9496–9508.
28. Jayasinghe, S. A., and Langen, R. (2005) Lipid membranes modulate the structure of islet amyloid polypeptide. *Biochemistry 44*, 12113–12119.
29. Apostolidou, M., Jayasinghe, S. A., and Langen, R. (2008) Structure of α-helical membrane-bound human islet amyloid polypeptide and its implications for membrane-mediated misfolding. *J. Biol. Chem. 283*, 17205–17210.
30. Nanga, R. P. R., Brender, J. R., Xu, J. D., Veglia, G., and Ramamoorthy, A. (2008) Structures of rat and human islet amyloid polypeptide IAPP(1−19) in micelles by NMR spectroscopy. *Biochemistry 47*, 12689–12697.
31. Landschulz, W. H., Johnson, P. F., and Mcknight, S. L. (1988) The leucine zipper: A hypothetical structure common to a new class of DNA-binding proteins. *Science 240*, 1759–1764.
32. Oshea, E. K., Rutkowski, R., and Kim, P. S. (1989) Evidence that the leucine zipper is a coiled coil. *Science 243*, 538–542.
33. Nilsson, M. R., and Raleigh, D. P. (1999) Analysis of amylin cleavage products provides new insights into the amyloidogenic region of human amylin. *J. Mol. Biol. 294*, 1375–1385.
34. Abedini, A., and Raleigh, D. P. (2005) Incorporation of pseudoproline derivatives allows the facile synthesis of human IAPP, a highly amyloidogenic and aggregation-prone polypeptide. *Org. Lett. 7*, 693–696.
35. Abedini, A., Singh, G., and Raleigh, D. P. (2006) Recovery and purification of highly aggregation-prone disulfide-containing peptides: Application to islet amyloid polypeptide. *Anal. Biochem. 351*, 181–186.
36. Levine, H. (1995) Thioflavine-T interaction with amyloid β-sheet structures. *Amyloid 2*, 1–6.
37. Westermark, G. T., Gebre-Medhin, S., Steiner, D. F., and Westermark, P. (2000) Islet amyloid development in a mouse strain lacking endogenous islet amyloid polypeptide (IAPP) but expressing human IAPP. *Mol. Med. 6*, 998–1007.
38. Meng, F., Marek, P., Potter, K. J., Verchere, C. B., and Raleigh, D. P. (2008) Rifampicin does not prevent amyloid fibril formation by human islet amyloid polypeptide but does inhibit fibril thioflavin-T interactions: Implications for mechanistic studies of β-cell death. *Biochemistry 47*, 6016–6024.
39. Jaikaran, E. T. A. S., Nilsson, M. R., and Clark, A. (2004) Pancreatic β-cell granule peptides form heteromolecular complexes which inhibit islet amyloid polypeptide fibril formation. *Biochem. J. 377*, 709–716.
40. Gilead, S., Wolfenson, H., and Gazit, E. (2006) Molecular mapping of the recognition interface between the islet amyloid polypeptide and insulin. *Angew. Chem., Int. Ed. 45*, 6476–6480.
41. Larson, J. L., and Miranker, A. D. (2004) The mechanism of insulin action on islet amyloid polypeptide fiber formation. *J. Mol. Biol. 335*, 221–231.
42. Westermark, P., Li, Z. C., Westermark, G. T., Leckstrom, A., and Steiner, D. F. (1996) Effects of β cell granule components on human islet amyloid polypeptide fibril formation. *FEBS Lett. 379*, 203–206.
43. Abedini, A., Meng, F., and Raleigh, D. P. (2007) A single-point mutation converts the highly amyloidogenic human islet amyloid polypeptide into a potent fibrillization inhibitor. *J. Am. Chem. Soc. 129*, 11300.

44. Yan, L. M., Tatarek-Nossol, M., Velkova, A., Kazantzis, A., and Kapurniotu, A. (2006) Design of a mimic of nonamyloidogenic and bioactive human islet amyloid polypeptide (IAPP) as nanomolar affinity inhibitor of IAPP cytotoxic fibrillogenesis. *Proc. Natl. Acad. Sci. U.S.A. 103*, 2046–2051.
45. Porat, Y., Mazor, Y., Efrat, S., and Gazit, E. (2004) Inhibition of islet amyloid polypeptide fibril formation: A potential role for heteroaromatic interactions. *Biochemistry 43*, 14454–14462.
46. Porat, Y., Abramowitz, A., and Gazit, E. (2006) Inhibition of amyloid fibril formation by polyphenols: Structural similarity and aromatic interactions as a common inhibition mechanism. *Chem. Biol. Drug Des. 67*, 27–37.
47. Scrocchi, L. A., Chen, Y., Wang, F., Han, K., Ha, K., Wu, L., and Fraser, P. E. (2003) Inhibitors of islet amyloid polypeptide fibrillogenesis, and the treatment of type-2 diabetes. *Lett. Pept. Sci. 10*, 545–551.
48. Aitken, J. F., Loomes, K. M., Konarkowska, B., and Cooper, G. J. S. (2003) Suppression by polycyclic compounds of the conversion of human amylin into insoluble amyloid. *Biochem. J. 374*, 779–784.
49. Buxbaum, J. N. (2009) Animal models of human amyloidoses: Are transgenic mice worth the time and trouble? *FEBS Lett. 583*, 2663–2673.
50. Butler, A. E., Jang, J., Gurlo, T., Carty, M. D., Soeller, W. C., and Butler, P. C. (2004) Diabetes due to a progressive defect in β-cell mass in rats transgenic for human islet amyloid polypeptide (HIP rat): A new model for type 2 diabetes. *Diabetes 53*, 1509–1516.
51. Yagui, K., Yamaguchi, T., Kanatsuka, A., Shimada, F., Huang, C. I., Tokuyama, Y., Ohsawa, H., Yamamura, K. I., Miyazaki, J. I., Mikata, A., Yoshida, S., and Makino, H. (1995) Formation of islet amyloid fibrils in β-secretory granules of transgenic mice expressing human islet amyloid polypeptide amylin. *Eur. J. Endocrinol. 132*, 487–496.
52. Fox, N., Schrementi, J., Nishi, M., Ohagi, S., Chan, S. J., Heisserman, J. A., Westermark, G. T., Leckstrom, A., Westermark, P., and Steiner, D. F. (1993) Human islet amyloid polypeptide transgenic mice as a model of non-insulin-dependent diabetes-mellitus (NIDDM). *FEBS Lett. 323*, 40–44.
53. Wong, W. P. S., Scott, D. W., Chuang, C. L., Zhang, S. P., Liu, H., Ferreira, A., Saafi, E. L., Choong, Y. S., and Cooper, G. J. S. (2008) Spontaneous diabetes in hemizygous human amylin transgenic mice that developed neither islet amyloid nor peripheral insulin resistance. *Diabetes 57*, 2737–2744.
54. Hull, R. L., Shen, Z. P., Watts, M. R., Kodama, K., Carr, D. B., Utzschneider, K. M., Zraika, S., Wang, F., and Kahn, S. E. (2005) Long-term treatment with rosiglitazone and metformin reduces the extent of, but does not prevent, islet antyloid deposition in mice expressing the gene for human islet antyloid polypeptide. *Diabetes 54*, 2235–2244.
55. Andrikopoulos, S., Hull, R. L., Verchere, B., Wang, F., Wilbur, S. M., Wight, T. N., Marzban, L., and Kahn, S. E. (2004) Extended life span is associated with insulin resistance in a transgenic mouse model of insulinoma secreting human islet amyloid polypeptide. *Am. J. Physiol. 286*, E862.
56. Henson, M. S., Buman, B. L., Jordan, K., Rahrmann, E. P., Hardy, R. M., Johnson, K. H., and O'Brien, T. D. (2006) An in vitro model of early islet amyloid polypeptide (IAPP) fibrillogenesis using human IAPP-transgenic mouse islets. *Amyloid 13*, 250–259.
57. Matveyenko, A. V., and Butler, P. C. (2006) Islet amyloid polypeptide (IAPP) transgenic rodents as models for type 2 diabetes. *ILAR J. 47*, 225–233.
58. Andrikopoulos, S., Verchere, C. B., Howell, W. M., Wight, T. N., and Kahn, S. E. (1998) Evidence for islet amyloid fibril formation in a new mouse model of insulinoma producing and secreting human islet amyloid polypeptide. *Diabetes 47*, A197.